# Study of structural and elastic properties of Nickel Oxide under high pressure up to 100 GPa using DFT method

Salah Tlili<sup>1</sup>, Belhadji Kinza Amel<sup>2</sup>, Terkhi Mohammed Cherif<sup>2</sup>, Mohammed Said Nedjimi<sup>3</sup>, Noura Mebrouki<sup>4</sup>, Ammar Haouat<sup>5</sup>

<sup>1</sup>Faculty of Mathematics and Material Sciences, Department of Physics, Development of New And Renewable Energies In Arid And Saharan Zones Laboratory (LENREZA), University of Ouargla, 30000 (Algeria)

<sup>2</sup>Faculty of Science and Technology, Department of Process Engineering, Laboratory of Environmental Sciences and Valorization Techniques (STEVA). University of Mostaganem, 27000 (Algeria)

<sup>3</sup>Faculty of Mathematics and Material Sciences, Department of Chemistry, Valorisation and Promotion of Saharan Resources Laboratory (VPRS), University of Ouargla, 30000 (Algeria)

<sup>4</sup>Faculty of Mathematics and Material Sciences, Department of Physics, Radiation and Plasmas and Surface Physics Laboratory (LRPPS), University of Ouargla, 30000 (Algeria) <sup>5</sup>Faculty of Exact Sciences, Department of Chemistry, University of El Oued, 39000 (Algeria)

Email: tlilisalah2007@gmail.com

This study aims to identify the extent of the effect of pressure on the structural and elastic properties of nickel oxide crystals, by changing it from 0 to 100 GPa. This study is computational using the DFT method, approximating GGA, as we chose the modern function PBEsol from among the multiple functions. Starting with the geometric optimization, we confirmed that the phase transformation of this oxide from phase B1 to phase R does not occur, i.e. this oxide remains stable in its first phase B1. Compared to previous studies, whether experimental or computational, especially at zero pressure, we found that the slight difference in the values of our results for the structural parameters, the derivative of the Bulk modulus confirms the validity of these results. This is despite the fact that the difference was large in the value of the Bulk modulus at this pressure, and we were not able to compare with the rest of the parameters.

Keywords: Nanostructure, DFT method, structural properties, elastic

properties, NiO.

## 1. Introduction

Nanostructure materials are receiving increased attention, and metal oxides such as NiO have received significant technological and industrial attention. This oxide is of great importance, including in many uses; Painting on ceramics, its role in fuel cell electrodes. Ferrite manufacturing processes (such as NiOFe<sub>2</sub>O<sub>3</sub>), which are used in the field of electronics. And because of its magnetic properties, it is used in the process of manufacturing nickel salts (such as chloride, nitrates and sulfates), which can be used to make refined nickel oxide. It is also used in the production process of active nickel catalysts, in electroplating, in stained glass and color removal. Nickel oxide (II) is also used in the ceramic industry, in order to make a combination of glazing, ferrite and ceramic coloring. This oxide in the form of sinter is also used in the production of steel and nickel alloys, and it also supplies oxygen to the melt to remove carbon as carbon dioxide. Some other important uses of nickel oxide (II) include the preparation of several nickel salts, specialized chemicals and nickel catalysts, used as an electrode in fuel cells [01].

Also during the early stages of the Earth's formation, there was a stage of differentiation where the Earth's constituent elements were separated into layers because of their density. Since nickel oxide is a metallic element, it may play a role in this process, as it is concentrated deep within the Earth. Nickel oxide is significantly involved in the formation of minerals, interacting with other elements, forming different metals, some of which are important in the Earth's crust. Studies have shown that nickel oxide is present in some meteorites and primitive materials that contributed to Earth's composition, understanding the distribution and amount of nickel in these materials can provide evidence of planetary formation processes [02].

This oxide is an inorganic compound containing Nickel (Ni) and Oxygen (O), it is a green cubic crystal that turns into an octa-surface shape black inclined to grey, known as black oxide and when it burns strongly, it becomes a black oxide with a metallic luster. Green oxide density 6.2 g/cm3 and it has a Mohs hardness of 5.5, it melts dissolves at 1955 °C. It is insoluble in water, but soluble in acids at normal temperatures. The black form of it dissolves in hot acids, noting that it appears in nature in the form of the mineral poinsettia, which is a solid chemical compound [03].

The structure of binary nickel oxide depends on the arrangement of nickel and oxygen atoms in the crystal lattice, this structure consists of Ni<sup>2+</sup> ions found in empty crystal lattice sites, surrounded by O<sup>2-</sup> ions that form cubes in the lattice. Nickel oxide is usually crystallized in a particular crystal structure, called fluorite crystals [04].

There are many works on the subject of nickel oxide, including experimentation, the most important of which; Work Noguchi, Y et.al 1998 [05], Shukla, A et.al 2002 [06], L. Liu et.al 2008 [07], Nwanya, A. C et.al 2015[08]and work Potapkin, V et.al 2016 [09]. Also computational ones, such as; de PR Moreira et.al 2002 [10], Zhang, W et al 2006 [11], Kuneš, J et.al 2007 [12] and Chauhan, Ret al 2008 [13]. While Gavriliuk, A. G et.al 2023 [14] worked on combining theory and practicality. Although these studies were of different

interest in several aspects, it can be concluded from most of them that;

This oxide in normal conditions, as a whole monoxides crystallize in the structure of Rooksalt or phase B1 (see figure (1)). This structure remains stable above 147 GPa as stated in the experimental study of Noguchi, Y et.al 1998 [05], where there is a possibility of it turning into the trigonal structure or the rhombohedral or R-3.It can also shift at very high pressures above 280 GPa to CsCl (B2) structure, as stated in the computational work of Chauhan, Ret al 2008 [13]. These structures are represented in figure (1) below, and their information is also recorded in the table below.

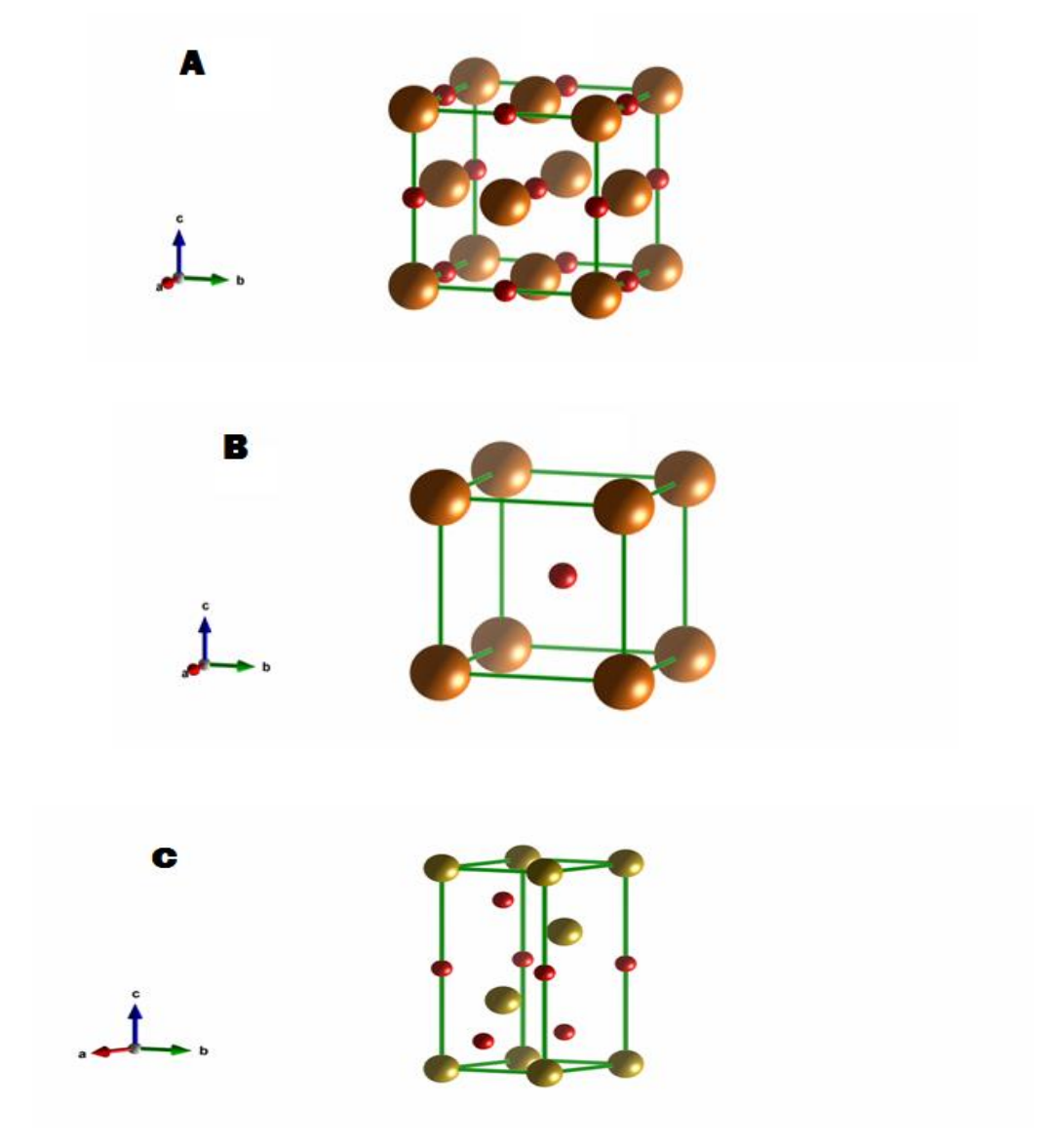


Figure (1): represents the possible crystal structures of nickel oxide prepared by the VESTA program, where balls are large in size and golden in color represent Ni<sup>2+</sup>. The balls are small

in size and red in color O<sup>2</sup>-.

- A- Cubic structure or structure of Rooksalt NaCl or phase B1 for oxide.
- B- Cubic structure or cesium chlorine structure represents CsCl or phase B2 for oxide.
- C- Trigonal structure or the rhombohedral or R-3 phase for oxide.

Table (1): Possible structural properties of nickel oxide, corresponding thermodynamic conditions

		conditions.			
structure	Cubic		Trigonal		
S-C	NaCl (B1)	CsCl (B2)	Rhombohedral		
G-S	Fm-3m	Pm-3m	R-3m		
N-G-S	225	221	166		
Z	8	8	1		
a	4.326/4.2506	4.2/4.24	2.95170		
В	4.326/4.2506	4.2/4.24	2.95170		
c	4.326/4.2506	4.2/4.24	7.21700		
α(°)	90	90	90		
β(°)	90	90	90		
γ(°)	90	90	120		
coor	Ni (0.0.0) O(0.5,0.5,0.5)	Ni (0.0.0) O(0.5,0.5,0.5)	Ni (0.0.0) O(0,0,0.5)		
Conditions	T=298 K, P=1atm	T=298 K, P=320 GPa	T=298 K, P=160 GPa		

These studies did not accurately determine the development of the values of many parameters, whether structural or elastic, especially within the scope of the first phase of this oxide.

Given the importance of many of these parameters, especially when using this oxide in nano fields. This paper came to provide information to the global data bank about the development of some of these parameters, in a computational way that simulates the hydraulic pressure of the material in a range starting from zero to 100 GPa. Therefore, this introduction is followed by a brief explanation of the study method, then an interpretation of the results and their presentation, and finally a summary that presents the most important results obtained from it

# 2. Method of study:

Generally the method of determination is computational in its origin, if overcome by simulation. In order to be clearer, it can be divided into two sections, depending on the method of calculating the parameters studied. Which in turn is classified according into two types, as follows:

# II-1 The elementary parameters:

These are parameters that are calculated directly by simulation program, i.e. those calculated without our own intervention. The methods of calculating these elementary parameters are generally many, as the most commonly used methods are so-called "ab-initio" methods based on partial dynamics [15], methods based on statistical physics (vibration methods) [16] and methods based on thermodynamics [17].

For our part, we applied DFT (Density Functional Theory), which is one of the most

important methods used in theoretical physics and chemistry, and through which we can determine the properties of a multi-particle system, the total energy of the system, the electronic density of the orbits, and the physical and optic parameters of the material..... etc, and is one of the most commonly used methods in quantum calculations to solve the Schrodinger equation because of their applicability to diverse (multi-variable) systems [18]. The CASTEP code (Cambridge Total Energy Package) is based on this theory [19], which uses many approximation. We used the GGA (Generalized Gradient Approximation) [21-20], which has been developed and strengthened for its multiple uses, in 2008 the PBEsol approximation appeared, used here and explained in detail in [22]. We have adopted the borders of the region of Brillion 10 x 10 x 10 and cut-off energy estimated at 630 eV. These values enable to provide a very close calculation with very reliable results.

In this program, the first step in the calculation is called geometric optimization, which identifies a lot of elementary parameters, especially those of structural properties. There are many of them, and here we are concerned with: Enthalpy of formation or heat content, crystal lattice parameters and their volume and the volumetric mass of matter or its density.

The used CASTEP program can calculate elastic properties, this in a second step depends on the type of cell used in the previous step. If this is done based on the elementary cell, the calculation is in less time. And that's what we did at all, where it was possible to notice that the results of the previous step cared about the elementary cell than terminological cell. This program has been developed in such a way that it can calculate a lot of parameters based primarily on calculating the parameters of elasticity, calculated from the Hawke's low [23]. Using special relationships as we will see later calculate elastic modulus; bulk modulus, shear modulus and averaged sound velocity.

# II-2 The complementary parameters:

These are the parameters that are not calculated by the program used, i.e. those for which we have to use other software tools to calculate their values. They are calculated based on the previous parameters. Here we are only interested in the volume ratio, which is considered the only complementary parameter within the structural properties. As for the elastic properties, we focused here on the propagation speeds of both longitudinal and transverse waves, which are considered among the most important parameters studied, especially in seismology. In addition to the speed of the acoustic compression wave, this can be calculated as we will see later.

#### II-3 Identification of reference structure:

Before all that, a reference structure for this program must be provided or built into it in order to start the calculation, by searching the Internet for sites that provide such a structure. It is preferable to choose the structure resulting from experimental studies rather than the one resulting from calculation, due to the realism of experimentation over calculation. Mostly, these sites provide the studied crystal structure in the works presented in the form of files with various extensions, from which we choose files with the extension cif. We also prefer to choose the most recent works, because they provide more accurate results.

# 3. Results and interpretation:

# III-1 Structural properties:

#### III-1-1 Phase transition and stable structures:

Change in the free energy  $\Delta G$  to form crystals that are equal to the  $\Delta H$  or Enthalpy formation at absolute zero [24], where:

$$\Delta G = \Delta H + T \Delta S = \Delta H + (0) \Delta S = \Delta H \tag{1}$$

where T temperature and  $\triangle S$  entropy forming.

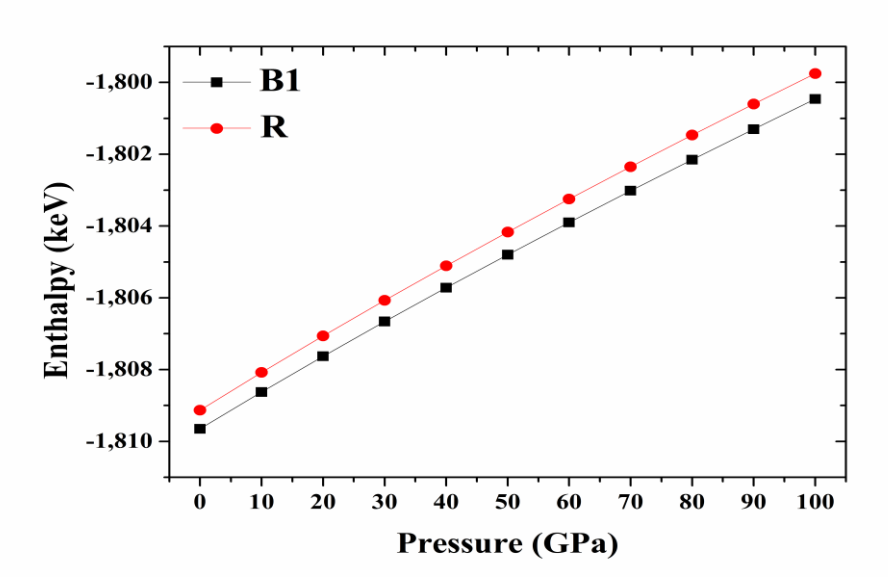


Figure (2): Change the Enthalpy of formation to form two structures of NiO with pressure up to 100 GPa.

Figure (2) Enthalpy of formation change of NiO crystal for B1 and R with pressure up to 100 GPa.

Through this form, the increased thermal content of the formation of the NiO crystal in its B1 and R phases, this is within two different and very similar areas of change, is observed. The presentation of a change in value for the first phase is estimated at 9.19 ev, while the estimate is 9.38 ev for the second phase, which means that the velocity of growth in the first phase is lower. The increase for both phases is almost linear, as their tendency is the same value divided by 100 GPa. On the other hand, this amount is always lower in the whole range of study than in the second phase. This shows that the B1 phase is stable. This is consistent with all previous studies, which determine that the periodic transformation is within the pressure of 147 GPa, in particular the work of [05] who decided it experimentally.

## III-1-2 The parameter structure and cell volume:

Where figure (3) shows the change of the primary crystal lattice parameter of NiO oxide by

the change of pressure up to 100 GPa, and also presents in table (1) some of the values of this parameter in the most important values of the studied pressure.

From figure (3) and table (2) note that the lattice parameter of stable phase decreases as pressure increases, this is within a range estimated to be width 0.11 A. But this decrease is not linear in the whole areas of study. If it is considered linear over the entire range, the slope of this decrease is estimated at  $1.10\ 10^{-3}\ A/GPa$ . In fact the line of change appears in the two range, the first of which is between 0 and 50 GPa and the second is between 60 and 100 GPa. The slope of the first range is estimated at  $1.24\ 10^{-3}\ A/GPa$ , while that of the second range is estimated at  $9.41\ 10^{-4}\ A/GPa$ .

The value of this parameter at 0 GPa converges with those resulting from what was decided in the experimental work [05], which it exceeds by 0.39 A.

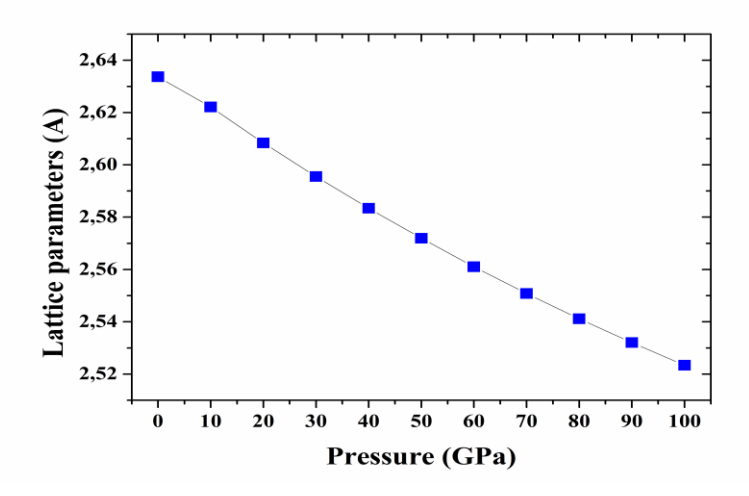


Figure (3): Change the lattice parameter for elementary cell of NiO in B1 phase with pressure up to 100 GPa.

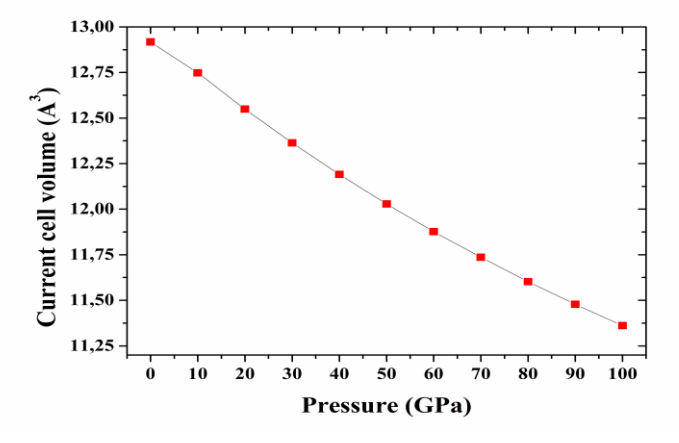


Figure (4): Change the elementary cell volume of NiO in B1 phase with pressure up to 100 *Nanotechnology Perceptions* Vol. 20 No.6 (2024)

GPa.

Figure (4) shows the change in elementary cell volume of NiO oxide by change in pressure up to 100 GPa, generally calculated from the following relationship:

$$V = \vec{a}.(\vec{b} \wedge \vec{c}) \tag{2}$$

Through figure (4), there is also a decrease in the volume of the elementary cell by increasing pressure, in fact cannot be linear, given the relationship that requires that there is a direct proportionality between this volume and the cubic crystal lattice parameter of oxide. But considering that its change is almost linear, it has the following slopes; 15.57  $10^{-3}$  A<sup>3</sup>/GPa on each study areas, 17.78  $10^{-3}$  A<sup>3</sup>/GPa in between 0 and 50 GPa 12.91  $10^{-3}$  A<sup>3</sup>/GPa between 60 and 100 GPa. The change in the entire areas of study is within the range of presentation of 1.56 A<sup>3</sup>, and for more information, the values of this volume are included at the most important limits of the study in line 4 of the table in table (2).

At 0 GPa the value of this volume is close with those resulting from what was decided in the experimental work [08], where it exceeds by 0.76 A<sup>3</sup>.

#### III-1-3 The volume ratio and stats function:

The volume ratio is calculated by dividing the volume of the cell at a given pressure on the volume of the cell at 0 pressures  $V_0$ , which is applicable in our study. That is, with the following relationship:

$$V_{ratio} = \frac{V(P)}{V_0} \tag{3}$$

The results of the calculation are represented in figure (5) presented for the change of this ratio at the pressures studied up to the pressure of 100 GPa and some values specified in table (2), from which it can be seen that the width of the range of change of this ratio is 0.12. Although there is no linearity in the decrease of this ratio over the entire study areas, the slope of this can be estimated at 1.21 10<sup>-3</sup>, and the linearity is more pronounced in the two previously approved ranges with slopes, respectively; 1.38 10<sup>-3</sup> and 10<sup>-3</sup>.

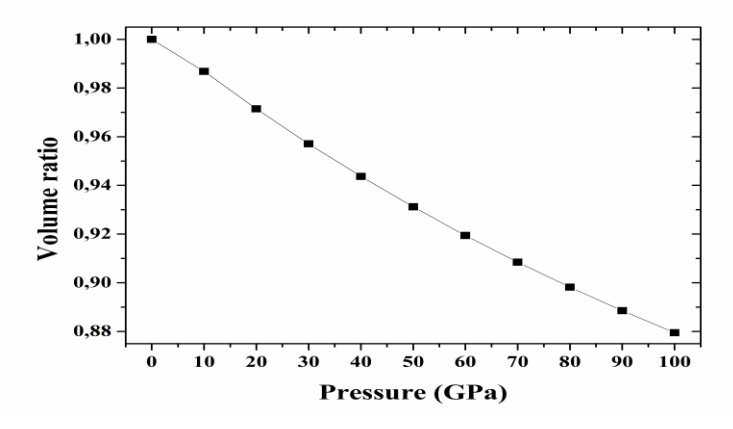


Figure (5): Change the volume ratio of NiO in B1 phase with pressure up to 100 GPa.

The change in pressure by the meaning of this parameter presents the equation of state, the most important of which is based on the definition of Barch-Markahan [25] and provided as follows:

$$P = \frac{3B_0}{2} \left[ \left( \frac{V}{V_0} \right)^{-\frac{7}{3}} - \left( \frac{V}{V_0} \right)^{-\frac{5}{3}} \right] \left[ 1 + \frac{3}{4} (B_0' - 4) \left( \left( \frac{V}{V_0} \right)^{-\frac{2}{3}} - 1 \right) \right]$$
(4)

This equation enables the determination of the value of bulk modulus B and its derived B " = dB/dP at 0 pressure.

After calculating the equation of state and using the values calculated by the program, we found that the values of both the bulk modulus and its derivative, respectively, are; 628.5 GPa and 3.28. Comparing the results of our calculations by the program to previous studies, the value of the bulk modulus mentioned is much higher than those mentioned in the experimental work [05]. It is more than five times superior, there is a clear incompatibility. The derivative value is 0.72 less than those published in the same work, and this difference is consistent.

# III-1-4 Study Density:

Figure (5) represents the density changes of phase B1 of the oxide depending on the pressure change within the study's limits.

Density or volumetric mass are also among the parameters provided by the program directly used in our accounts, which are calculated in monoxides as follows:

In the case of the NaCl structure, using the following relationship:

$$\rho = 6.64 \frac{M_O + M_{Ni}}{V_C} \tag{5}$$

where: V<sub>C</sub> the conventional cell volume is taken in a cubic centimeter unit.

Table (2): values of Enthalpy of formation, crystal lattice parameter, elementary cell volume and volume ratio and density of NiO at some study limits.

Pressure (GPa)	0	50	60	100
Enthalpy of formation for R phase (kev)	-1,809654	-1,80480077	-1,80390081	-1,80046145
Enthalpy of formation for B1 phase (kev)	-1,80913034	-1,80416679	-1,80234904	-1,79975131
lattice parameter of elementary cell (A)	2,633735	2,57189	2,561029	2,523372
Elementary cell volume (A <sup>3</sup> )	12,918179	11,877598	11,877598	11,361326
Volume ratio	1	0,9311959	0,9194483	0,8794836
Density (g/cm3)	5,18079	5,563587	5,634672	5,890718

Through figure (6) it can be observed that the density at 10 GPa and pressure whose value is 5.25 g/cm<sup>3</sup>, deviates slightly from the change of the rest of the values. With the exception of this value or without regard to its simple deviation, it can be considered that this change in density is increasing almost linearly by an estimated slope 7.1 10<sup>-3</sup> g/cm<sup>3</sup>.GPa. But between 0 and 50 GPa is this increase is faster as the slope is estimated at 7.66 10<sup>-3</sup> g/cm<sup>3</sup>.GPa, while between 60 and 100 GPa the increase is slower as the slope is estimated at 6.40 10<sup>-3</sup> g/cm<sup>3</sup>.GPa. This change in density on each areas of study is within an estimated range of width of 0.71 g/cm<sup>3</sup>, by comparing the value resulting from our study, it converges with that

of the experimental study at work [05], which exceed our value by 1.63 g/cm<sup>3</sup>.

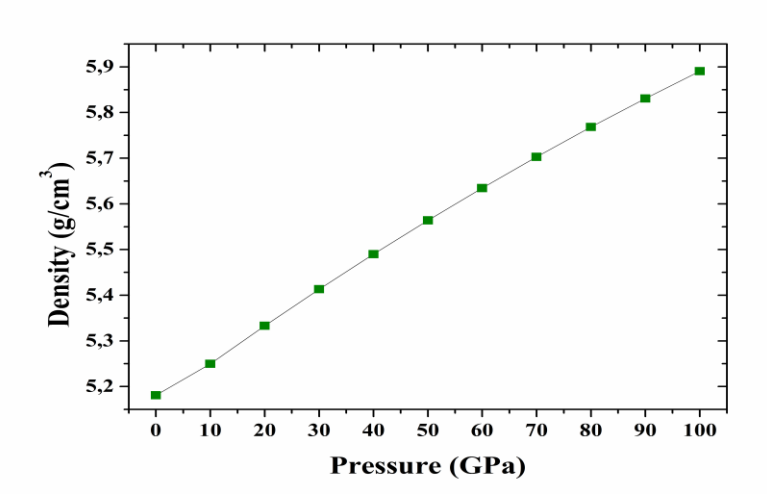


Figure (6): Change the Density of NiO in B1 phase with pressure up to 100 GPa.

# III-2 Study the elastic properties:

## III-2-1 The elastic constants:

The elastic constants of materials provide a link between mechanical and dynamic behavior of crystals, and give important information regarding the nature of forces affecting on solids [23].

For cube symmetry, it identifies the three constants  $C_{11}$ ,  $C_{12}$  and  $C_{44}$ .

Figure (7) represents elasticity constant variations  $C_{11}$ ,  $C_{12}$  and  $C_{44}$  to NiO crystal in its phase B1 with pressure change up to 100 GPa. This shows that there has been a change in the whole area of study limited within areas that are respectively estimated at 746.23, 266.65 and GPa 23.01. This change is clearly linear in the three constants, increasing for  $C_{11}$  and  $C_{12}$  While this change is decreasing with the emergence of a type of stability for  $C_{44}$ , this has slopes equal to the supply amounts divided by 100 (see table (3)). Unfortunately, values for these constants were not available in previous studies at 0 GPa, to compare them with the results of our study.

Among the many benefits of calculating elastic constants, we can calculate the conditions for confirming the stability of the crystal or not. These conditions are given in the case of the cubic crystal system with the following relationships [26]:

$$Condition 1 = C_{11} + 2C_{12} + P (6)$$

$$Condition 2 = C_{44} - P \tag{7}$$

$$Condition3 = C_{11} - C_{12} - 2P (8)$$

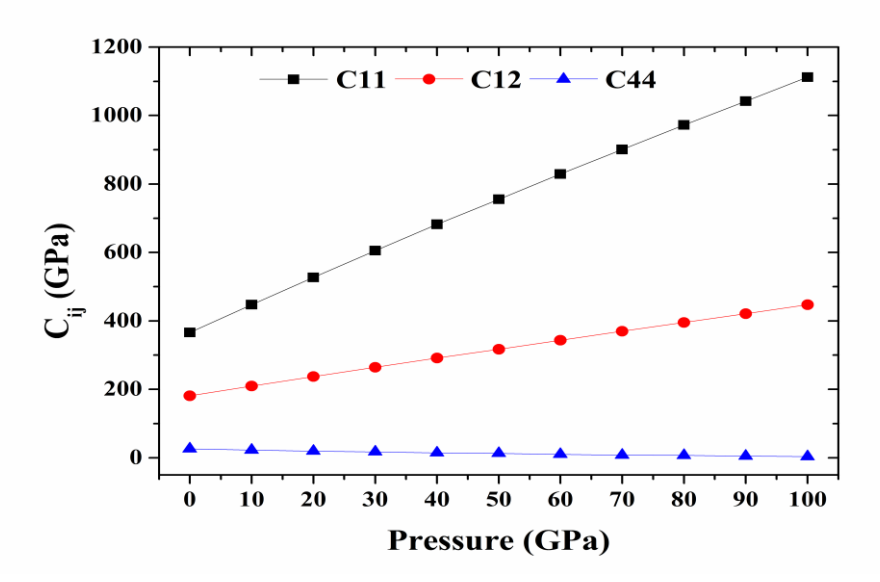


Figure (7): Change the elasticity constants  $C_{11}$ ,  $C_{12}$  and  $C_{44}$  of NiO in B1 phase with pressure up to 100 GPa.

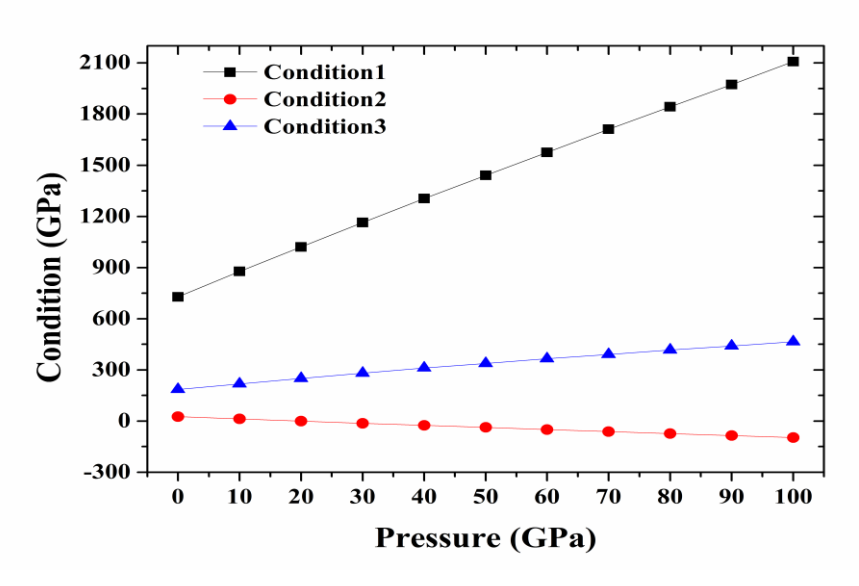


Figure (8): Change the stability conditions of NiO in B1 phase with pressure up to 100 GPa.

Figure (8) gives the evolution of NiO crystal stabilization conditions through elasticity constants when increasing pressure up to 100 GPa, this figure calculated its values through crystal stability confirmation conditions that uses elasticity constants through the above relationships. This figure shows an increase in the first and third conditions, while the second requirement decreases. Nevertheless, the increase in the first condition is faster by slope

estimated to 13.80, as opposed to the third condition slope is 2.80. While there is a slowdown in the second condition, this is a slope of 1.23, this confirms what has already been achieved in relation to the stability of the crystallization of this oxide in the phase B1, which is the result obtained when studying Enthalpy formation or thermal content.

## III-2-2 The modulus elastics:

The bulk modulus (B) is a measure of the resistance of a material to compression when an external pressure is applied to that material. It is also known as the inverse relationship of compressibility [27], while the shear modulus is also called the torsional modulus (Shear modulus) and is symbolized by G [28].

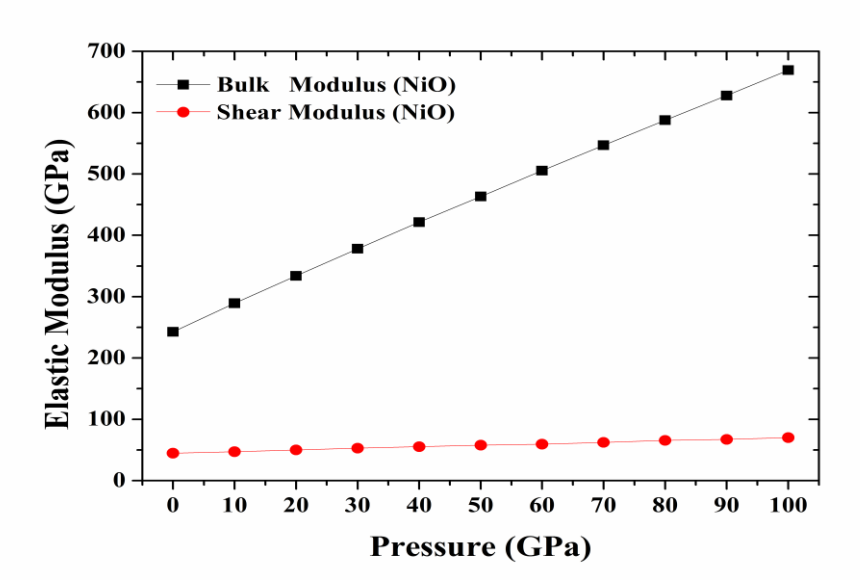


Figure (9): Change the bulk modulus B and shear modulus G of NiO in B1 phase with pressure up to 100 GPa.

Figure (9) represents changes in the elastic modulus: the bulk modulus and the shear modulus of NiO crystallization in its phase B1 by the evolution of pressure up to 100 GPa is evident from the continuous increase in both two parameters along the limits of the study, where they displayed their respective area of change and at a succession estimated at 426.51 and 25.33 GPa. Similarly, it is evident from the same figure that a change in the bulk modulus is much faster than a change in the shear modulus, with the slope to change each over the entire study range estimated at 4.27 and 0.25 (see table (3)). Also, for these two parameters, no values were available in previous studies at least at 0 pressure, to compare them with our findings.

## III-2-3 The elastic waves velocities:

By knowing the density values studied in the previous chapter and shear modulus values can be calculated the transversal wave velocity, depending on the following relationship [28]:

$$V_{\rm S} = \sqrt{\frac{G}{\rho}} \tag{9}$$

But by adding the values of the bulk modulus, the longitudinal wave velocity can be calculated, as follows:

$$V_p = \sqrt{\frac{3B + 4G}{3\rho}} \tag{10}$$

The bulk sound wave velocity can be concluded from the knowledge of the values of density and the bulk modulus, which is written as follows:

$$V_{\varphi}^2 = \frac{B}{\rho} \tag{11}$$

It can also be calculated from knowing the values of longitudinal and transversal wave velocity, through the following relationship:

$$V_{\varphi}^2 = V_p^2 - \frac{4}{3}V_s^2 \tag{12}$$

The same values as the longitudinal and transversal wave velocity can be calculated as the averaged sound velocity, depending on the following relationship:

$$V_a = \left[\frac{1}{3} \left(\frac{2}{V_s^3} + \frac{1}{V_n^3}\right)\right]^{-\frac{1}{3}} \tag{13}$$

Table (3): Constants elastic values, elastic modulus and waves velocities studied for NiO at some study limits.

	2			
Pressure (GPa)	0	50	60	100
Constant elastic C <sub>11</sub> (GPa)	366,3571	755,64975	829,25725	1112,5851
Constant elastic C <sub>12</sub> (GPa)	180,8367	317,25435	343,2938	447,4884
Constant elastic C <sub>44</sub> (GPa)	26,23395	12,61955	9,8588	3,2193
Bulk modulus (GPa)	242,67683	463,38615	505,28162	669,1873
Shear modulus (GPa)	44,81566	57,752911	59,5529	70,14124
Longitudinal wave velocity (km/s)	5,99834	6,61363	6,67837	7,09868
Transversal wave velocity (km/s)	2,94115	3,22188	3,251	3,45066
Bulk sound wave velocity (km/s)	4,94432	5,46804	5,52346	5,87496
Averaged sound velocity (km/s)	2,7028	2,28839	2,12286	1,48833

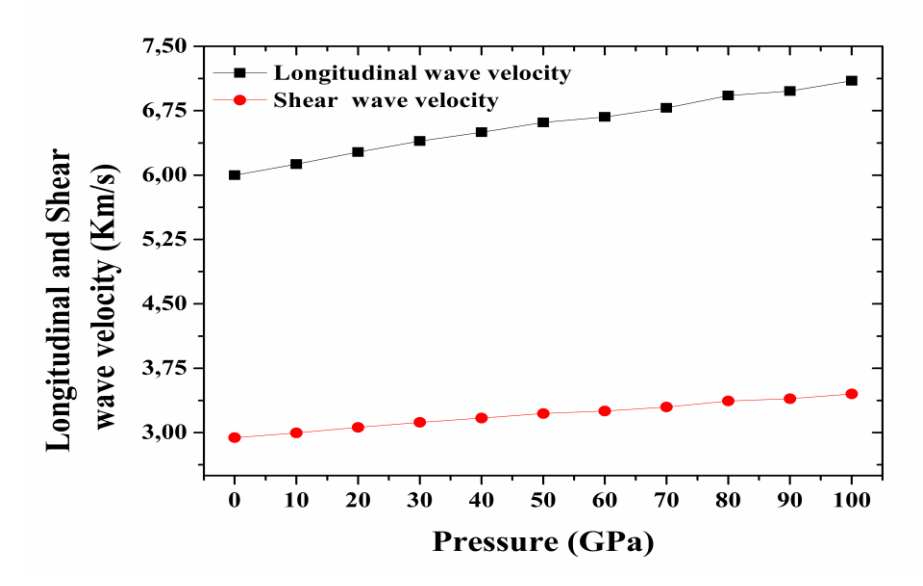


Figure (10): Change the longitudinal V<sub>P</sub> and transversal V<sub>S</sub> wave velocities of NiO in B1 phase with pressure up to 100 GPa.

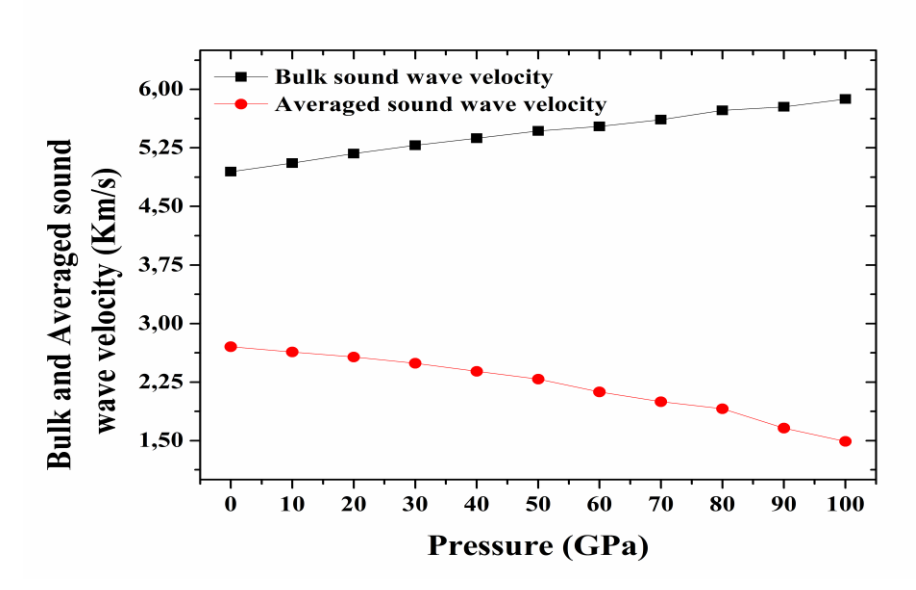


Figure (11): Change the Averaged  $V_a$  and Bulk  $V_{\phi}$  sound wave velocities of NiO in B1 phase with pressure up to 100 GPa.

Figure (10) shows the change in longitudinal and transversal wave velocity of nickel oxide by the change of pressure up to 100 GPa, while figure (11) represents the bulk sound wave velocity and the wave of the acoustic deviation in the same oxide and in the same conditions of pressure change. Through the two figures, it is clear that with increasing pressure, the

velocities longitudinal, transversal and bulk sound wave increase, while averaged sound velocity values decrease.

In the total area these velocities change in ranges with a width that are respectively estimated at 1.10, 0.51, 0.93, and 1.21 km/s. Change over the whole area, however the velocity, is non-linear, but may also be considered as such in two ranges, which are the same two ranges mentioned in the previous chapter. The first range is between 0 and 50 GPa, with slopes estimated at 12.31 10<sup>-3</sup>, 5.61 10<sup>-3</sup>, 10.47 10<sup>-3</sup> and 8.29 10<sup>-3</sup> km/GPa.s. However, the second range is between 60 and 100 GPa, with the exception of the values of all velocities at 80 GPa slightly deviated from linearity, the slopes are estimated at 10.51 10-3, 4.99 10-3, 8.79 10-3 and 15.86 10-3 km/GPa.s. It can also be noted that the velocity values of the bulk sound wave velocity are greater than those of the Averaged sound velocity, and this is evident through the values recorded in Table (3). These values we get are not comparable to other values from previous studies, and this is a view of their unavailability.

#### 4. Conclusion:

The calculation gives many parameters, which we considered as primary parameters, namely; crystal parameter, elementary cell volume and density as structural properties and elastic constants, bulk and shear modulus as part of the elastic properties. As for the volume ratio as the last structural parameter and the velocity of elastic or seismic waves as a remaining part of the elastic properties, we considered them complementary parameters, because they are calculated based on laws that can be programmed with ease.

Through this work, we have been able to find:

- That the oxide in our study area does not undergo a phase transition, as it remains stable in its first phase B1, which is consistent with previous computational and experimental studies.
- Most studied parameters are increasing with increased pressure, except for both; Structural characteristics parameters in which only density is increasing, elasticity constant  $C_{44}$  and averaged sound velocity.
- At absolute zero the values of our study results correspond only to the values of structural properties, the velocity of changing the values of the bulk modulus with the change of pressure. While the value of the bulk modulus itself is very far away, with our inability to compare the rest of the parameters values due to their unavailability.

In the future, we could suggest the number of research directions, which always fall within this range, as follows:

- Re-study in a more accurate way, by choosing another functional dependent, especially since nickel is considered a magnetic material.
- The study can be directed to apply its results within a certain range, such as by studying the possibility of oxidation in the Earth's layers.
- The results of this study can be invested to calculate other parameters, the Young's modulus, Poisson4 ratio... etc as elastic properties. It can also continue studying other properties, such as thermodynamic properties.

## References

- [01] Huheey, J. E., Keiter, E. A., Keiter, R. L., & Medhi, O. K. (2006). Inorganic chemistry: principles of structure and reactivity. Pearson Education India.
- [02] Barnes, C. E. (2003). Inorganic chemistry (catherine e. housecroft and alan g. sharpe). Journal of Chemical Education, 80(7), 747.
- [03] Poirier, J. P. (2000). Introduction to the Physics of the Earth's Interior. Cambridge University Press.
- [04] Cornell, R. M., & Schwertmann, U. (2003). The iron oxides: structure, properties, reactions, occurrences, and uses (Vol. 664). Weinheim: Wiley-vch.
- [05] Noguchi, Y., Uchino, M., Hikosaka, H., Kusaba, K., Fukuoka, K., Mashimo, T., & Syono, Y. (1998). Shock compression of NiO to 130 GPa. The Review of High Pressure Science and Technology, 7, 832-834.
- [06] Shukla, A., Rueff, J. P., Badro, J., Vanko, G., Mattila, A., de Groot, F. F., & Sette, F. (2003). Charge transfer at very high pressure in NiO. Physical Review B, 67(8), 081101.
- [07] Liu, L., Li, X. D., Liu, J., Jiang, S., Li, Y. C., Shen, G. Y., ... & Xu, J. (2008). High pressure structural and elastic properties of NiO up to 67 GPa. Journal of Applied Physics, 104(11).
- [08] Nwanya, A. C., Offiah, S. U., Amaechi, I. C., Agbo, S., Ezugwu, S. C., Sone, B., ... & Ezema, F. I. (2015). Electrochromic and electrochemical supercapacitive properties of room temperature PVP capped Ni (OH) 2/NiO thin films. Electrochimica Acta, 171, 128-141.
- [09] Potapkin, V., Dubrovinsky, L., Sergueev, I., Ekholm, M., Kantor, I., Bessas, D., ... & Abrikosov, I. A. (2016). Magnetic interactions in NiO at ultrahigh pressure. Physical Review B, 93(20), 201110
- [10] de PR Moreira, I., Illas, F., & Martin, R. L. (2002). Effect of Fock exchange on the electronic structure and magnetic coupling in NiO. Physical Review B, 65(15), 155102.
- [11] Zhang, W. B., Hu, Y. L., Han, K. L., & Tang, B. Y. (2006). Pressure dependence of exchange interactions in NiO. Physical Review B—Condensed Matter and Materials Physics, 74(5), 054421.
- [12] Kuneš, J., Anisimov, V. I., Skornyakov, S. L., Lukoyanov, A. V., & Vollhardt, D. (2007). NiO: correlated band structure of a charge-transfer insulator. Physical review letters, 99(15), 156404.
- [13] Chauhan, R., & Singh, S. (2008). Structural study of Novel (superhard) material: NiO. Pramana, 70, 307-311.
- [14] Gavriliuk, A. G., Struzhkin, V. V., Ivanova, A. G., Prakapenka, V. B., Mironovich, A. A., Aksenov, S. N., ... & Morgenroth, W. (2023). The first-order structural transition in NiO at high pressure. Communications Physics, 6(1), 23.v
- [15] Marx, D., & Hutter, J. (2000). Ab initio molecular dynamics: Theory and implementation. Modern methods and algorithms of quantum chemistry, 1(301-449), 141.
- [16] Radovic, M., Lara-Curzio, E., & Riester, L. (2004). Comparison of different experimental techniques for determination of elastic properties of solids. Materials Science and Engineering: A, 368(1-2), 56-70.
- [17] Kumar, M. (2002). Application of high pressure—high temperature equation of state for elastic properties of solids. Physica B: Condensed Matter, 311(3-4), 340-347.
- [18] Hohenberg, P., & Kohn, W. J. P. R. (1964). Density functional theory (DFT). Phys. Rev, 136(1964), B864.
- [19] Segall, M. D., Lindan, P. J., Probert, M. A., Pickard, C. J., Hasnip, P. J., Clark, S. J., & Payne, M. C. (2002). First-principles simulation: ideas, illustrations and the CASTEP code. Journal of physics: condensed matter, 14(11), 2717.
- [20] Perdew, J. P., & Zunger, A. (1981). Self-interaction correction to density-functional approximations for many-electron systems. Physical review B, 23(10), 5048.
- [21] Perdew, J. P., Burke, K., & Ernzerhof, M. (1996). Generalized gradient approximation made simple. Physical review letters, 77(18), 3865.

- [22] Perdew, J. P., Ruzsinszky, A., Csonka, G. I., Vydrov, O. A., Scuseria, G. E., Constantin, L. A., ... & Burke, K. (2008). Restoring the density-gradient expansion for exchange in solids and surfaces. Physical review letters, 100(13), 136406.
- [23] Sahraoui, F. A., Arab, F., Zerroug, S., & Louail, L. (2008). First-principles study of structural and elastic properties of MgSe under hydrostatic pressure. Computational materials science, 41(4), 538-541.
- [24] Tlili, S., Louail, L., Bouguera, A., Haddadi, K., & Medkour, Y. (2017). Contribution to the study of structural and elastic properties of wüstite under pressure up to 140 GPa by pseudopotential calculations. Phase Transitions, 90(12), 1229-1240.
- [25] Birch, F. (1978). Finite strain isotherm and velocities for single-crystal and polycrystalline NaCl at high pressures and 300 K. Journal of Geophysical Research: Solid Earth, 83(B3), 1257-1268.
- [26] Hachemi, A., Saoudi, A., Louail, L., Maouche, D., & Bouguerra, A. (2009). Elasticity of the B2 phase and the effect of the B1–B2 phase transition on the elasticity of MgO. Phase Transitions, 82(1), 87-97.
- [27] Ahmad, J. F., & Mhmood, Z. R. (2020). Study the Effect of High Pressure and High Temperature on the Properties of Nacl-B1. Journal of Education and Science, 29(2), 101-117.
- [28] Jeanloz, R., & Knittle, E. (1989). Density and composition of the lower mantle. Philosophical Transactions of the Royal Society of London. Series A, Mathematical and Physical Sciences, 328(1599), 377-389.